

## Indirect magnetic interaction mediated by a spin dimer in $\text{Cu}_2\text{Fe}_2\text{Ge}_4\text{O}_{13}$

T. Masuda,<sup>1,\*</sup> K. Kakurai,<sup>2</sup> M. Matsuda,<sup>2</sup> K. Kaneko,<sup>3</sup> and N. Metoki<sup>3</sup>

<sup>1</sup>International Graduate School of Arts and Sciences, Yokohama City University, Yokohama, Kanagawa, 236-0027, Japan

<sup>2</sup>Quantum Beam Science Division, JAEA, Tokai, Ibaraki 319-1195, Japan

<sup>3</sup>Advanced Science Research Center, JAEA, Tokai, Ibaraki 319-1195, Japan

(Received 26 March 2007; published 1 June 2007)

$\text{Cu}_2\text{Fe}_2\text{Ge}_4\text{O}_{13}$  is a bicomponent compound that consists of Cu dimers and Fe chains with separate energy scale. By inelastic neutron scattering technique with high-energy resolution we observed the indirect Fe-Fe exchange coupling by way of the Cu dimers. The obtained parameters of the effective indirect interaction and related superexchange interactions are consistent with those estimated semistatically. The consistency reveals that the Cu dimers play the role of nonmagnetic media in the indirect magnetic interaction.

DOI: [10.1103/PhysRevB.75.220401](https://doi.org/10.1103/PhysRevB.75.220401)

PACS number(s): 75.10.Jm, 75.25.+z, 75.50.Ee

Some types of magnetic interaction in solid are *indirect* ones by way of nonmagnetic media. The superexchange interaction among the most common type in insulating metal oxides is derived by perturbative treatment of electron transfer between nonmagnetic anions and magnetic ions.<sup>1</sup> Another type is found in Ruderman-Kittel-Kasuya-Yoshida (RKKY) interaction in magnetic alloys<sup>2</sup> where free electrons in the nonmagnetic metal transfer exchange integral between magnetic atoms. Anions or nonmagnetic metal behaves as the media for the indirect interaction. As the exotic types spin-singlet entities such as spin dimers, ladders, spin integer chains<sup>3</sup> can play a similar role. The theoretical treatment was considered in nonmagnetic impurity doped  $S=1$  chains,<sup>4,5</sup>  $S=1/2$  ladders,<sup>6,7</sup> or  $S=1/2$  dimerized chains.<sup>8,9</sup> Around the impurity the induced staggered spins generate an effective spin of  $S=1/2$  in the sea of nonmagnetic state. The low energy excitation are described by the effective spins that indirectly interact with the similar formula to the RKKY interaction. This scenario is experimentally realized in doped spin gap compounds such as  $\text{CuGeO}_3$ ,<sup>10</sup>  $\text{SrCu}_2\text{O}_3$ ,<sup>11</sup> and  $\text{PbNi}_2\text{V}_2\text{O}_8$ .<sup>12</sup> However, randomness of the impurity distribution makes the system rather complex. For the basic understanding a bicomponent spin compound with uniformly distributed magnetic ions is necessary.

Recently, Fe-doped  $\text{CuGeO}_3$  with uniform Fe distribution was identified in insulating metal oxide  $\text{Cu}_2\text{Fe}_2\text{Ge}_4\text{O}_{13}$ ;  $\text{Cu}_{n-2}\text{Fe}_2\text{Ge}_n\text{O}_{3n+1}$  with  $n=4$  in a hypothetical series of homologous structures with  $n=3, 5, 6, \dots, \infty$ .<sup>13</sup> Here the compound with  $n=\infty$  corresponds to well known spin-Peierls cuprite  $\text{CuGeO}_3$  (Ref. 10), where uniform 1D chains of  $\text{Cu}^{2+}$  ions run in the  $c$  direction as is illustrated in Fig. 1(a). In  $\text{Cu}_2\text{Fe}_2\text{Ge}_4\text{O}_{13}$  50% of  $\text{Cu}^{2+}$  ( $S=1/2$ ) ions are periodically replaced by  $\text{Fe}^{3+}$  ( $S=5/2$ ) and the uniform chains become distorted alternating chains of  $S=1/2$  and  $S=5/2$  dimers in Fig. 1(b). Consequently, the lattice unit is quadrupled along the chain direction and the  $c$  axis in  $\text{CuGeO}_3$  changes to the  $a$  axis in  $\text{Cu}_2\text{Fe}_2\text{Ge}_4\text{O}_{13}$ . Bulk susceptibility and neutron inelastic scattering (NIS) measurements indicated that the  $J_{\text{Cu-Fe}}$  are weak<sup>14-17</sup> and, instead, the strength of the interdimer interaction of Fe ions ( $J'_b$ ) is the same as that of the intradimer one ( $J_b$ ) within the experimental error. Hence,  $\text{Cu}_2\text{Fe}_2\text{Ge}_4\text{O}_{13}$  is a weakly coupled quantum dimers of Cu ions and classical uniform chains of Fe ions in the  $b$  direc-

tion. In this geometry Cu dimers seem to behave as nonmagnetic media for effective exchange interaction ( $J_{\text{eff}}$ ) of neighboring Fe ions as is described in Fig. 1(c). A set of exchange parameters were determined by NIS and neutron diffraction (ND) in the previous study as is summarized in the first line of Table I. In spite of the rigorous experiments the direct measurement of  $J_{\text{eff}}$  was not performed because of the twinning of the available crystal. The values in the square bracket is the reference estimates by a semistatic method.

In this paper we performed cold neutron inelastic scattering experiment with high-energy resolution on the twinned but high-quality crystal. Through elaborate data analysis we successfully obtained the low energy excitation in the  $a^*$  direction where the  $J_{\text{eff}}$  makes a main contribution. We analyze whole dispersion in combination with previously reported data<sup>17</sup> by both the conventional spin wave (SW) and the effective SW model based on the energy scale separation. We found the latter model more appropriate in quantitative level. The obtained consistency between the  $J_{\text{eff}}$ 's estimated by the dynamics measurement and the semistatic method reveals that the Cu dimers play the role of the nonmagnetic media in the indirect interaction between Fe spins.

The high quality crystal with the dimension of  $7 \times 5 \times 40 \text{ mm}^3$  was obtained by floating zone method. NIS experiment was performed on LTAS spectrometer installed in JRR-3 in JAEA. Open-80'-80'-open with soller collimation and fixed final energy of  $E_f=3.5 \text{ meV}$  were employed. Closed He cycle refrigerator was used to achieve  $T=3.0 \text{ K}$ . The crystal structure of  $\text{Cu}_2\text{Fe}_2\text{Ge}_4\text{O}_{13}$  is monoclinic. The obtained crystal was twinned so that  $a^*$  and  $b^*$  axes are shared as is illustrated in Fig. 1(d). Here the reciprocal spaces for crystal A and B are defined as  $a^*b^*c^*$  (dashed grid) and  $a'^*b'^*c'^*$  (dashed dotted grid) coordinates, respectively. In  $\text{Cu}_2\text{Fe}_2\text{Ge}_4\text{O}_{13}$  a reciprocal vector  $(h \ k \ l)$  in crystal A corresponds to  $(-(h+0.53l) \ -k \ l)$  in crystal B. The  $a^*b^*c^*$  coordinate will be used hereafter.

A series of constant  $q$  scans were performed on the trajectory of the thick solid line in Fig. 1(d). Peak profiles of the typical scans are shown in Fig. 2(a). At antiferromagnetic zone center of  $h=2.0$ , well-defined spin wave excitation with an anisotropy gap of about 1 meV was observed in crystal A. The peak is wider than experimental resolution and seems to

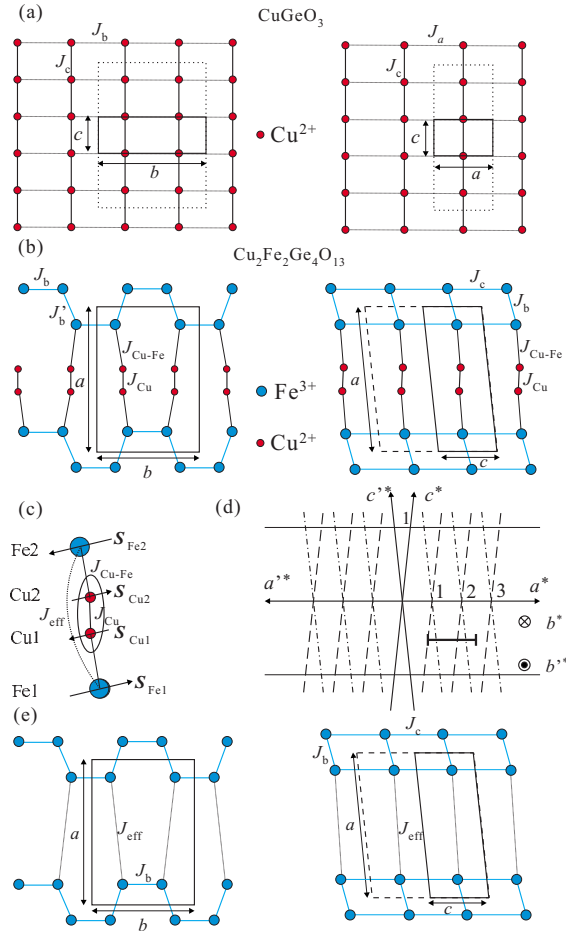


FIG. 1. (Color online) (a) Schematic structure of  $\text{CuGeO}_3$  projected onto  $c$ - $b$  (left panel) and  $c$ - $a$  (right panel) planes. (b) Schematic structure of  $\text{Cu}_2\text{Fe}_2\text{Ge}_4\text{O}_{13}$ . Lattice unit cell and magnetic unit cell are shown by solid and dashed lines, respectively. Main exchange path is crank-shaft Fe chains along  $b$  direction and Cu dimers. (c) Indirect Fe-Fe coupling by way of Cu dimers. (d) The structure of the twinned crystal of  $\text{Cu}_2\text{Fe}_2\text{Ge}_4\text{O}_{13}$  projected onto the  $a^*$ - $c^*$  plane. Dot-dashed and dashed grids are for crystal A and B, respectively. (e) Schematic structure of  $\text{Cu}_2\text{Fe}_2\text{Ge}_4\text{O}_{13}$  based on the effective SW model (see text).

have a structure probably due to  $xy$  two ion anisotropy. The shape of the scan profiles are well explained by considering resolution function in the Cooper-Nathans approximation<sup>18</sup> that is shown by solid curves. At  $\hbar\omega \sim 2.4$  meV, broad peak from crystal B is detected. These two peaks move with the change of  $h$  on the identical trajectories shown by dashed-dotted and dashed curves. We fitted the data by a pair of

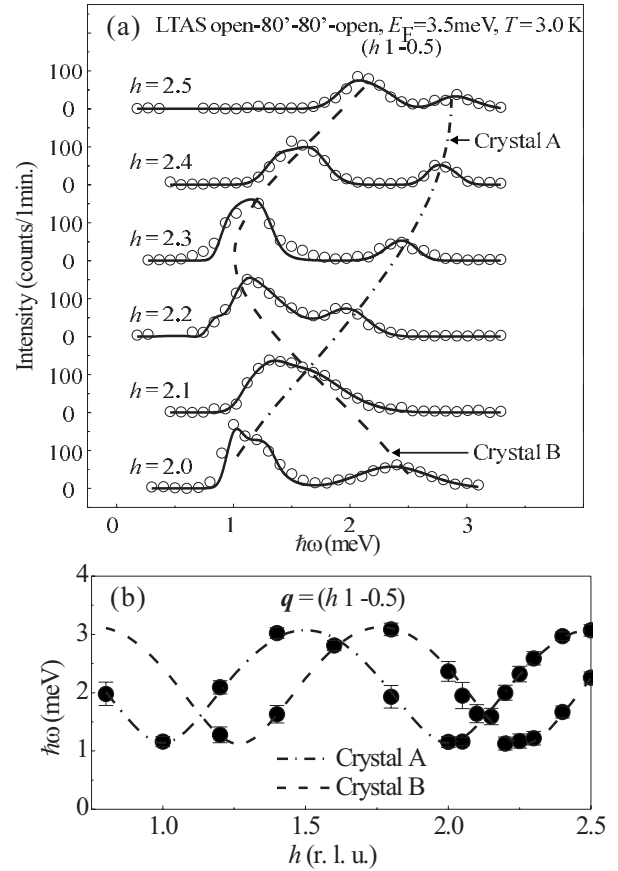


FIG. 2. (a) Constant  $q$  scans at  $(h \ 1 \ -0.5)$ . The dashed-dotted and dashed curves indicate excitations from crystal A and B, respectively. Solid curves are fitting curves by resolution convoluted function. (b) Dispersion curves of crystal A (dashed-dot) and crystal B (dashed).

simple Gaussian functions and we obtained the dispersion relations in Fig. 2(b). Two curves from crystals A and B are separately observed, which are identical by translational displacement of  $h' = -(h + 0.53l)$ . Thus the dispersion in the  $a^*$  direction with the boundary energy of about 3 meV is successfully obtained in  $\text{Cu}_2\text{Fe}_2\text{Ge}_4\text{O}_{13}$ . In combination with the previous data<sup>17</sup> the whole dispersions in three independent directions are drawn in Fig. 3(a). Filled symbols are the data by single crystal NIS and the gray shaded area around 24 meV is a narrow band excitation observed in powder NIS experiment.

In the first scenario we analyze the data by the conventional SW model. Since all the spins are confined in almost

TABLE I. Exchange parameters for  $\text{Cu}_2\text{Fe}_2\text{Ge}_4\text{O}_{13}$  determined by neutron inelastic scattering (NIS) and neutron diffraction (ND). The values in the square bracket are the estimates by the semistatic method.

	$J_{\text{Cu}}$ (meV)	$J_b$ (meV)	$J_c$ (meV)	$J_{\text{eff}}$ (meV)	$J_{\text{Cu-Fe}}/J_{\text{Cu}}$	$J_{\text{Cu-Fe}}$ (meV)	$\Delta$ (meV)
NIS and ND (Refs. 14 and 17)	$2.4(2) \times 10$	1.60(2)	0.12(1)	[0.13(4)]	[0.10(5)]	[2.4(2)]	
NIS (Conventional SW)	$2.(4) \times 10^2$	1.59(2)	0.13(2)			0.9(6)	1.0(5)
NIS (Effective model)		1.59(2)	0.13(2)	0.09(6)		2.0(5)	1.0(5)

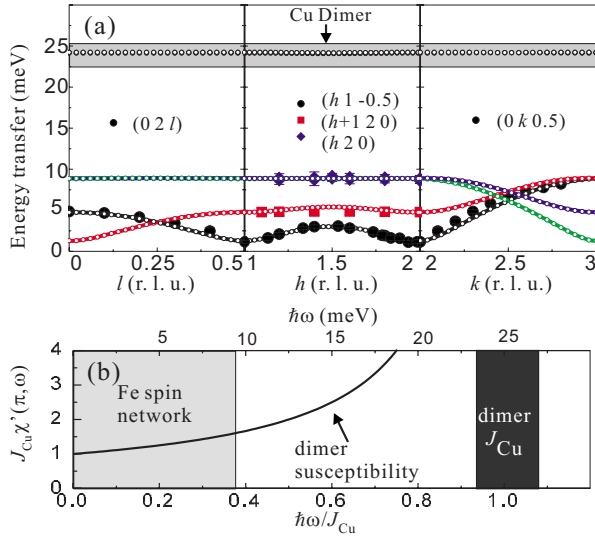


FIG. 3. (Color online) (a) The dispersion relation in  $\text{Cu}_2\text{Fe}_2\text{Ge}_4\text{O}_{13}$ . The lower energy excitation in  $a^*$  direction (filled circles) is determined in the current study. Other data are from Ref. 17. Solid lines and small open circles are the fit by conventional SW and effective SW model (see text). (b) Energy scales of Fe chains and Cu dimers. Dynamic susceptibility of dimers is indicated by a solid curve.

$a$ - $c$  plane and the canting is small,<sup>14</sup> we start from collinear structure. We assume isotropic interactions for Fe-Fe, Cu-Fe, and Cu-Cu spins for the simplicity. Hence the Hamiltonian is defined as

$$\mathcal{H} = \frac{1}{2} \sum_{\substack{\alpha, \beta, \gamma \in 8 \text{ Fe sublattices,} \\ \delta, \epsilon, \zeta \in 8 \text{ Cu sublattices}}} (J_{\alpha\beta} \mathbf{S}_\alpha^{\text{Fe}} \cdot \mathbf{S}_\beta^{\text{Fe}} + J_{\gamma\delta} \mathbf{S}_\gamma^{\text{Fe}} \cdot \mathbf{T}_\delta^{\text{Cu}} + J_{\epsilon\zeta} \mathbf{T}_\epsilon^{\text{Cu}} \cdot \mathbf{T}_\zeta^{\text{Cu}}). \quad (1)$$

Here  $\alpha$ ,  $\beta$ , and  $\gamma$  denote Fe sublattices and  $\delta$ ,  $\epsilon$ , and  $\zeta$  denote Cu sublattices.  $\mathbf{S}^{\text{Fe}}$  and  $\mathbf{T}^{\text{Cu}}$  are the spin operators of  $S=5/2$  and  $S=1/2$  on Fe and Cu ions, respectively. We considered  $J_b$ ,  $J_c$ ,  $J_{\text{Cu-Fe}}$ , and  $J_{\text{Cu}}$  in Fig. 1(b) as the contributed exchange parameters in Eq. (1). In addition the split anisotropy gaps  $\Delta_x$  and  $\Delta_y$  are empirically introduced as  $[\hbar\omega_{x,y}(\mathbf{q})]^2 = [\hbar\omega(\mathbf{q})]^2 + \Delta_{x,y}^2$ .  $\Delta_{x,y} = 0.95$  and  $1.16$  meV were obtained by fitting the resolution convoluted function to the constant  $q$  scan at  $\mathbf{q} = (2 \ 1 \ -0.5)$ , where the  $xy$  anisotropy is the most enhanced. The split is small enough and we will use the mean value  $\Delta = 1.0(5)$  meV as fixed parameter hereafter.

The numerical fit to the dispersion is indicated by small open circles in Fig. 3(a). The fit to the data is very good.

While doing simulation it is found that dispersionless excitation at  $\hbar\omega \sim 24$  meV, where four modes are overlapped, is sensitive to the change of parameter  $J_{\text{Cu}}$ . This means that they are from Cu centered spins. Similarly, four modes in the lower energy are from Fe centered spins. The estimated exchange parameters relating to Fe spins are summarized in the second line in Table I. They are reasonably consistent with previously estimated values in the first line. However,  $J_{\text{Cu}}$  of  $2.6 \times 10^2$  meV is very different from the previous value 24.2 meV in Ref. 17. This is because of the different assumption for the ground state; classical Néel state for the present SW and singlet dimer state for the previous analysis. To discuss the  $J_{\text{Cu}}$ , the isostructural compound  $\text{Cu}_2\text{Sc}_2\text{Ge}_4\text{O}_{13}$ ,<sup>15</sup> where Fe ions in Fig. 1(b) are replaced by nonmagnetic Sc ions would give good insight. In these compounds the angle  $\angle \text{Cu-O-Cu}$  and the bond distance are very close to each other and so would the magnitude of superexchange constant be. The intradimer interaction in  $\text{Cu}_2\text{Sc}_2\text{Ge}_4\text{O}_{13}$  was reliably determined as  $J_{\text{Sc}} = 24.5 \sim 25.4$  meV by the isolated dimers model.<sup>16</sup> The value is close to the previous estimate of  $J_{\text{Cu}}$  24.2 meV (Ref. 17) rather than the present one  $2.6 \times 10^2$  meV. Hence, the singlet dimer ground state is a better assumption and we adopt the  $J_{\text{Cu}} = 24.2$  meV as the reasonable value hereafter.

In the second scenario we will consider the effective SW model based on the energy scale separation of the magnetic excitations.<sup>17</sup> The absence of dispersion in the Cu centered mode and the suppressed magnetic moment means that Cu spins are strongly bound to spin dimers singlet state. Onto the Cu1 spin in the dimer the field  $h_{\text{Cu1}}$  is applied through  $J_{\text{Cu-Fe}}$  by the Fe1 spins in Fig. 1(c). Then the polarized spins  $S_{\text{Cu}} = \chi(\pi, \omega) h_{\text{Cu}}$ , are induced on the both Cu1 and Cu2 ions that transfer the exchange integral from one Fe spin to another. Here the dynamic susceptibility of the dimer  $\chi(\pi, \omega)$  is purely real and expressed by  $\chi(\pi, \omega) = 1/(J_{\text{Cu}} - \hbar\omega)$  at  $T = 0$  K [solid curve in Fig. 3(b)]. In the energy region of Fe spin networks (gray shaded area)  $\chi(\pi, \omega)$  is almost  $1/J_{\text{Cu}}$  and constant. This suggests that static treatment of MF-RPA works well when we consider the spin dynamics at  $\hbar\omega \lesssim 10$  meV. Then the indirect coupling  $J_{\text{eff}}$  can be approximately expressed as  $J_{\text{eff}}(\omega) = J_{\text{Cu-Fe}}^2 \chi(\pi, \omega) / 2 \sim J_{\text{Cu-Fe}}^2 / 2J_{\text{Cu}}$ . Thus the effective spin Hamiltonian for the low energy region is

$$\mathcal{H} = \frac{1}{2} \sum_{\alpha, \beta \in 8 \text{ Fe sublattices}} J_{\alpha\beta} \mathbf{S}_\alpha^{\text{Fe}} \cdot \mathbf{S}_\beta^{\text{Fe}}. \quad (2)$$

We considered  $J_b$ ,  $J_c$ , and  $J_{\text{eff}}$  as the exchange parameters as is illustrated in Fig. 1(e). The calculated dispersion relation is

$$[\hbar\omega(\mathbf{q})]^2 = \begin{cases} S^2 \{ (A^2 - D^2) - (B^2 + C^2 + 2BC \cos \pi k) \pm 2D \sqrt{B^2 + C^2 + 2BC \cos \pi k} \}, \\ S^2 \{ (A^2 - D^2) - (B^2 + C^2 - 2BC \cos \pi k) \pm 2D \sqrt{B^2 + C^2 - 2BC \cos \pi k} \}. \end{cases} \quad (3)$$

Here  $A=2J_b+J_{\text{eff}}+2J_c$ ,  $B=\sqrt{J_b^2+J_{\text{eff}}^2+2J_bJ_{\text{eff}}\cos 2\pi h}$ ,  $C=J_b$ , and  $D=2J_c\cos 2\pi l$ . Reasonable fit to the data is shown by the thick solid curves in Fig. 3(a). They are perfectly overlapped on the open small circles calculated in the first scenario. The obtained exchange parameters are summarized in the third line in Table I.

Excellent consistency was found in the independently estimated exchange parameters of Fe-centered spins. Particularly interesting is the effective indirect coupling  $J_{\text{eff}}$ 's. In the current study we obtained  $J_{\text{eff}}=0.09(6)$  meV by the direct measurement of the spin dynamics. In the previous study<sup>14</sup>  $J_{\text{Cu-Fe}}/J_{\text{Cu}}$  was estimated statically in MF-RPA level from the staggered magnetization curves of Cu dimers obtained by ND. Combining the parameter with  $J_{\text{Cu}}=24.(2)$  meV in a separate experiment,<sup>17</sup>  $J_{\text{eff}}=0.13(4)$  meV was estimated semistatically. The reasonable consistency in  $J_{\text{eff}}$ 's means that the static MF-RPA treatment works well and, thus, Cu dimers behave as the nonmagnetic media in the indirect Fe-Fe coupling. Due to the simplicity of the model, all the related exchange constants,  $J_{\text{Cu}}$ ,  $J_{\text{eff}}$ , and  $J_{\text{Cu-Fe}}$  are experimentally obtained.

There are a few other compounds reported as bicomponent systems with spin-singlet entity and additional spin. Among them  $R_2\text{BaNiO}_5$  ( $R$ =rare earth metals) have been studied the most in detail.<sup>19</sup> The compound is described by reasonably decoupled one dimensional  $\text{Ni}^{2+}$  ( $S=1$ ) chains and surrounding rare earth ions. The weak coupling induce

magnetically ordered state of which the nature is similar to that in  $\text{Cu}_2\text{Fe}_2\text{Ge}_4\text{O}_{13}$ .<sup>20</sup> However, the rare earth moment behaves as Ising type spin and the indirect interaction by way of Haldane chains has not been studied. Other examples are  $\text{Cu}_2\text{CdB}_2\text{O}_6$  and  $\text{Cu}_3(\text{P}_2\text{O}_6\text{OH})_2$ .<sup>21</sup> Spin model of quantum dimers and nearly free spins is proposed from the observed magnetization plateaux in the  $M$ - $H$  curves. For lack of single crystal, however, the detailed spin dynamics is still unknown. As far as we know  $\text{Cu}_2\text{Fe}_2\text{Ge}_4\text{O}_{13}$  is the only model compound for the indirect magnetic interaction by way of spin singlet media.

In conclusion we succeeded to obtain the spin dispersion in the  $a^*$  direction in  $\text{Cu}_2\text{Fe}_2\text{Ge}_4\text{O}_{13}$  by high-resolution neutron scattering experiment and by the elaborate data analysis. The whole dispersion is well explained by the effective SW model. The effective Fe-Fe interaction  $J_{\text{eff}}$  is directly estimated and the value is consistent with that obtained semistatically. It is found that  $\text{Cu}_2\text{Fe}_2\text{Ge}_4\text{O}_{13}$  is a prototype compound for randomness-free RKKY-like interaction in insulating metal oxides.

We wish to acknowledge fruitful discussion with A. Zheludev in the early stage of this study. C. Yasuda is appreciated for useful comments. This work was supported by the grant for Strategic Research Project No. W17003, No. K17028, and No. K18032 of Yokohama City University, Japan.

\*Email address: tmasuda@yokohama-cu.ac.jp

<sup>1</sup>P. W. Anderson, Phys. Rev. **100**, 564 (1959).

<sup>2</sup>M. A. Ruderman and C. Kittel, Phys. Rev. **96**, 99 (1954); T. Kasuya, Prog. Theor. Phys. **16**, 45 (1956); K. Yoshida, Phys. Rev. **106**, 893 (1957).

<sup>3</sup>F. D. M. Haldane, Phys. Lett. **93A**, 464 (1983).

<sup>4</sup>I. Affleck, T. Kennedy, E. H. Lieb, and H. Tasaki, Phys. Rev. Lett. **59**, 799 (1987).

<sup>5</sup>S. Miyashita and S. Yamamoto, Phys. Rev. B **48**, 913 (1993).

<sup>6</sup>H. Fukuyama, N. Nagaosa, M. Saito, and T. Tanimoto, J. Phys. Soc. Jpn. **65**, 2377 (1996).

<sup>7</sup>M. Sigrist and A. Furusaki, J. Phys. Soc. Jpn. **65**, 2385 (1996).

<sup>8</sup>H. Fukuyama, T. Tanimoto, and M. Saito, J. Phys. Soc. Jpn. **65**, 1182 (1996).

<sup>9</sup>C. Yasuda, S. Todo, M. Matsumoto, and H. Takayama, Phys. Rev. B **64**, 092405 (2001).

<sup>10</sup>M. Hase, I. Terasaki, and K. Uchinokura, Phys. Rev. Lett. **70**, 3651 (1993).

<sup>11</sup>M. Azuma, Z. Hiroi, M. Takano, K. Ishida, and Y. Kitaoka, Phys. Rev. Lett. **73**, 3463 (1994).

<sup>12</sup>Y. Uchiyama, Y. Sasago, I. Tsukada, K. Uchinokura, A. Zheludev, T. Hayashi, N. Miura, and P. Böni, Phys. Rev. Lett. **83**, 632 (1999).

<sup>13</sup>T. Masuda, B. C. Chakoumakos, C. L. Nygren, S. Imai, and K. Uchinokura, J. Solid State Chem. **176**, 175 (2003).

<sup>14</sup>T. Masuda, A. Zheludev, B. Grenier, S. Imai, K. Uchinokura, E. Ressouche, and S. Park, Phys. Rev. Lett. **93**, 077202 (2004).

<sup>15</sup>G. J. Redhammer and G. Roth, J. Solid State Chem. **177**, 2714 (2004).

<sup>16</sup>T. Masuda and G. J. Redhammer, Phys. Rev. B **74**, 054418 (2006).

<sup>17</sup>T. Masuda, A. Zheludev, B. Sales, S. Imai, K. Uchinokura, and S. Park, Phys. Rev. B **72**, 094434 (2005).

<sup>18</sup>M. J. Cooper and R. Nathans, J. Appl. Crystallogr. **23**, 357 (1967).

<sup>19</sup>A. Zheludev, J. P. Hill, and D. J. Buttrey, Phys. Rev. B **54**, 7216 (1996).

<sup>20</sup>A. Zheludev, E. Ressouche, S. Maslov, T. Yokoo, S. Raymond, and J. Akimitsu, Phys. Rev. Lett. **80**, 3630 (1998); A. Zheludev, S. Maslov, T. Yokoo, S. Raymond, S. E. Nagler, and J. Akimitsu, J. Phys.: Condens. Matter **13**, R525 (2001).

<sup>21</sup>M. Hase, M. Kohno, H. Kitazawa, O. Suzuki, K. Ozawa, G. Kido, M. Imai, and X. Hu, Phys. Rev. B **72**, 172412 (2005); M. Hase, M. Kohno, H. Kitazawa, N. Tsujii, O. Suzuki, K. Ozawa, G. Kido, M. Imai, and X. Hu, *ibid.* **73**, 104419 (2006).